Third International Conference on Sustainable Construction Materials and Technologies http://www.claisse.info/Proceedings.htm

Corrosion Behavior of Polyolefin Fiber Cement-based Composites Containing Supplementary Cementitious Materials

Wei-Ting Lin[1,2*], Yuan-Chieh Wu[1], Yu-Chih Chen[1,3], An Cheng[2] and Ran Huang[4]

[1]*Institute of Nuclear Energy Research, Atomic Energy Council, Executive Yuan, Taiwan*
[2]*Dept. of Civil Engineering, National Ilan University, Taiwan*
[3]*Institute of Aeronautics and Astronautics, National Cheng Kung University, Taiwan*
[4]*Dept. of Harbor and River Engineering, National Taiwan Ocean University, Taiwan*
[*]*No. 1000, Wenhua Rd., Jiaan Village, Longtan Township, Taoyuan County, 32546, Taiwan, e-mail address: wtlin@niu.edu.tw*

ABSTRACT

In this study, the impressed voltage corrosion and the impressed current corrosion test are conducted to evaluate the corrosion behavior of composites with different addition of polyolefin fiber, ultrafine slag, silica fume or mixed cementitious materials. Test results indicate that a little amount of polyolefin fibers can extend the time of chlorine ion reach to the surface of rebar and decrease the rebar corrosion. However, the fiber is not very useful for corrosion resistance of steel when the chlorine ions reach the surface of rebar and corrode it. In addition, the inclusion of ultrafine slag or silica fume can arrest the rebar corrosion and improve the compactness through pozzolanic reactivity and filling effects. According to the corrosion behavior and economy performance of the composites, the combination of 55 % ultrafine slag, 5 % silica fume and 0.8 % polyolefin fibers provided the best corrosion resistance of the tested cement-based composites.

Keywords. Impressed Voltage Corrosion Test, Corrosion Current, Polyolefin Fiber

INTRODUCTION

In general, the constituents of cement-based composites include cementitious material, water, aggregate and/or additives. Fiber is one of the commercially available additives and has been added in cement-based composites since 1960 to enhance composite properties, particularly tensile strength, abrasion resistance and energy absorbing capacity (Chalioris, 2009; kang, 2011). The presence of fiber refrains the growth or propagation of internal cracks and helps to transfer load (Şahin, 2011). The composites with fiber have much higher ductility than those without fiber, and demonstrate a significant increase in energy absorption or toughness (Lin, 2008). However, this represents a relatively short period in which to conduct such studies, and most efforts have focused on mechanical properties rather than the durability of fiber reinforced concrete (Passuello, 2009; Asokan, 2010). Polyolefin fiber is a kind of chemical synthetic fiber, which can equably disperse in concrete and has high corrosion resistance to acid, alkali and salt, so it has been incrementally applied in

engineering. Polyolefin chemical fibers demonstrate good performance in flexural fatigue strength, ductility toughness, and impact resistance (Han, 2012). At present, the research of polyolefin fiber cement-based composites mainly focuses on the mechanical properties; however, few studies have evaluated the combination of polyolefin fibers and supplementary cementitious materials mixed into cement-based composites. They are also non-corrosive, non-magnetic, and do not result in hazardous protrusions. Nonetheless, further research into the durability of these products is urgently required for applications in coastal areas and cold climates requiring the application of salt for deicing.

For many years, supplementary cementitious materials (SCMs) such as ultrafine slag abs silica fume have proven effective in minimizing the problems of durability include the creation of less permeable composites or denser pastes, which inhibit the propagation of cracks, and provide a cover of adequate thickness (Sahmaran, 2009; Lee, 2012). In addition, the cement-based composites containing SCMs and fibers are less permeable and well protected throughout its designed service life, the detrimental substances such as chloride ion, sulfate ion and acid can not easily penetrate into the composites, and thus the durability of structure is maintained. Moreover, many previous researchers have studied either polyolefin fibers or SCMs individually; however, few studies have evaluated the combination of polyolefin fibers and SCMs mixed into cement-based composites. This study evaluates the effects of ultrafine slag powders, silica fume and polyolefin fibers on the corrosion behavior of cement-based composites and investigates the relationship between replacement ratio of SCMs and corrosion index.

EXPERIMENTAL

Materials. This study used four fiber contents (0 %, 0.4 %, 0.8 % and 1.6 % by volume of total cement-based composites), three ultrafine slag contents (0 %, 40 % and 60 %) and three silica fume contents (0 %, 2 % and 5 % by weight of cement) in the mix design at the same water/cementitious (w/cm) ratios (0.55). Table 1 presents the chemical components of Type I Portland cement, ultrafine slag powders and silica fume. Ultrafine slag powder and silica fume with a fineness of 6000 cm^2/g and 22500 cm^2/g was used in powder form. The fineness modulus of fine aggregate was 2.82 and specific gravity of fine aggregate 2.02 g/cm^3. The maximum size of coarse aggregate was 25 mm and specific gravity of coarse aggregate 2.65 g/cm^3. The length of the polyolefin fibers was 25 mm with a diameter of 0.63 mm. The physical properties are shown in Table 2.

Table 1. Chemical Composition of Cement, Slag and Silica fume (% by mass)

Composition	SiO_2	Al_2O_3	Fe_2O_3	CaO	MgO	SO_3	K_2O	L. O. I. and others
Cement	20.9	5.6	3.1	63.4	2.9	2.4	0.4	1.3
Slag	33.5	14.0	0.4	41.6	6.9	0.7	1.1	1.8
Silica fume	91.5	0.2	0.7	0.4	1.5	0.5	1.9	3.3

Mix Proportion. For each mixture, all components (cement, ultrafine slag powders, polyolefin fibers, and aggregate) were mixed, cast, and vibrated in a sequence similar to that used for conventional concrete. The mix design is shown in Table 3. The coding used in the column is as follows: “PC” represent the control specimens at the w/cm ratio of 0.35; “G40” and “G60” represent the dosages of slag at 40 % and 60 %, respectively; “S2” and “S5”

represent the dosages of silica fume at 2 % and 5 %, respectively; and "4", "8" and "16" represent the dosages of polyolefin fibers at 0.4 %, 0.8 % and 1.6 %, respectively. The target slump was set to approximately 150 mm through the use of a high-range water-reducing admixture. Embedded #4 rebar was made of medium carbon steel according to ASTM A615 specifications

Table 2. Physical Properties of Polyolefin Fiber

Properties	Value and condition
Specific Gravity(Bulk Relative Density)	0.91
Tensile Strength	275 MPa
Modulus of Elasticity	2647 MPa
Elongation at Break	15 %
Ignition Point	593 ℃
Melt Point	160 ℃
Chemical and Salt Resistance	Excellent
Alkaline Resistance	Excellent
Electrical Conductivity	Low

Specimens. A total of twenty-eight different mixes (five hundred-four specimens) were cast as concrete specimens. For each mix, twelve ψ100 x 200 mm cylindrical specimens were used to test compressive strength. In addition, six ψ100 x 200 mm cylindrical specimens were prepared for the accelerated corrosion test and impressed voltage corrosion test, respectively.

Test Methods. Compressive strength test at ages of 7, 28, 56 and 91 days were performed in accordance with ASTM C39-12 to obtain the strength development curves of cement-bases composites containing silica fume and fibers.

For accelerated corrosion test, a 12.7 mm-diameter rebar was embedded in the center of the cylindrical specimen and the exposed surface area of rebar in 3.5 % NaCl solution was approximately 40 cm^2, controlled by epoxy-seal application as demonstrated in Fig. 1. The corrosion cell was connected so that #4 rebar acted as working electrode, saturated calomel electrode as reference electrode, and the titanium mesh as counter electrode. A current density of 0.5 mA/cm^2 was applied and the open circuit potential (OCP) and linear polarization resistance was measured using a Nichia NP-G100/ED potentiostat at a 24-hour interval. The polarization resistance (R_p) is generally related to a uniform corrosion rate and the polarization resistance measurements are accurate and rapid (Stren, 1957). The polarization resistance of the reinforcing steel is defined as the slope of the potential-current density curve at the zero current point when the rate of polarization is close to zero (ASTM G59, 2003):

$$R_p = [\frac{\partial(\Delta E)}{\partial i}]_{i=0, dE/dt \to 0} \quad (1)$$

where R_p is the polarization resistance ($K\Omega$-cm^2), ΔE is the applied potential (mV) and i is the current density (mA/cm^2). In this study, the applied external potential was increased or decreased gradually within ±10 mV at an interval of 20 mV and the corresponding currents

were measured. The polarization resistances were then calculated using the slope of the potential-current density curve. In addition, the corrosion current density (i_{corr}) can be estimated from Stern-Geary equation.

$$i_{corr} = \left[\frac{\beta_a \beta_c}{2.303(\beta_a + \beta_c)} \right] \times \frac{1}{R_p} = \frac{B}{R_p} \quad (2)$$

where i_{corr} is the corrosion current density, and β_a, β_c are the anodic and cathodic Tafel slopes, respectively. R_p is the polarization resistance. For iron, the constant, B, is assumed to be 26 mV in evaluating corrosion rate of steel for actively corroding system and 52 mV for passively system. After the corrosion current density is obtained, the instantaneous corrosion rate (r) can be calculated from Faraday's law as follows:

$$r = \frac{i_{corr}}{n} \times \frac{a}{F} \quad (3)$$

where F is Faraday's constant (96500 coulombs/equivalent), n is the number of equivalent exchange, and a is the atomic weight.

The same illustration with the accelerated corrosion test was used in the impressed voltage corrosion test, which is accordance with NT BUILD 356-89. A direct current with a potential of 15 V was maintained in this testing. In addition, the corrosion current of every reservoir saved by a data logger at every 10 min and corrosion current-time figures were drawn at the accelerated corrosion test system.

RESULTS AND DISCUSSION

Compressive Strength. Fig. 2 shows the development of compressive strength in the specimens. Specimens prepared with ultrafine slag powders demonstrated lower compressive strength than the control specimens at 7 days, but exceeded the control specimens at 28 days. Because the pozzuolana activity of ultrafine slag powders was less than that of cement, the initial reaction rate was lower. The ultrafine slag powders contained more SiO_2 and Al_2O_3, prompting a secondary hydration reaction with the cement hydration product $Ca(OH)_2$, to produce C-S-H and C-A-H, increase the compactness of the slag concrete, and enhance its compressive strength. The compressive strength of specimens with polyolefin fibers and those with silica fume increased, compared to the control specimens, proportional to the quantity of fibers and silica fume added. Specimens combining ultrafine slag powders or silica fume with polyolefin fibers demonstrated superior performance to specimens containing individual constituents of slag, silica fume or fibers. The presence of SCMs helped to strengthen the bond between the fibers and matrix. It is clear that the filling effect and pozzolanic activity of SCMs improves the strength and pore structure of polyolefin fiber cement-based composites. Moreover, the specimens combining fibers with slag and silica fume enhanced better compressive strength than other specimens containing individual constituents of slag, silica fume or fibers, which provide an effective barrier against the development of cracks under axial loading. In conclusion, the combination of 35 % ultrafine slag, 5 % silica fume and 0.8 % polyolefin fibers provided the best compressive strength of the tested cement-based composites.

Table 3. Mix Design (kg/m^3)

Mix no.	water	Coarse aggregate	Fine aggregate	cement	slag	Silica fume	Polyolefin fiber
PC	202	569	1006	367	0	0	0
PC4	202	569	1006	367	0	0	3.5
PC8	202	569	1006	367	0	0	7
PC16	202	569	1006	367	0	0	14
G40	202	569	1006	220	147	0	0
G404	202	569	1006	220	147	0	3.5
G408	202	569	1006	220	147	0	7
G4016	202	569	1006	220	147	0	14
G60	202	569	1006	147	220	0	0
G604	202	569	1006	147	220	0	3.5
G608	202	569	1006	147	220	0	7
G6016	202	569	1006	147	220	0	1.4
S2	202	569	1006	360	0	7	0
S24	202	569	1006	360	0	7	3.5
S28	202	569	1006	360	0	7	7
S216	202	569	1006	360	0	7	1.4
S5	202	569	1006	349	0	18	0
S54	202	569	1006	349	0	18	3.5
S58	202	569	1006	349	0	18	7
S516	202	569	1006	349	0	18	1.4
G35S5	202	569	1006	220	128	18	0
G35S54	202	569	1006	220	128	18	3.5
G35S58	202	569	1006	220	128	18	7
G35S516	202	569	1006	220	128	18	1.4
G55S5	202	569	1006	147	220	18	0
G55S54	202	569	1006	147	220	18	3.5
G55S58	202	569	1006	147	220	18	7
G55S516	202	569	1006	147	220	18	1.4

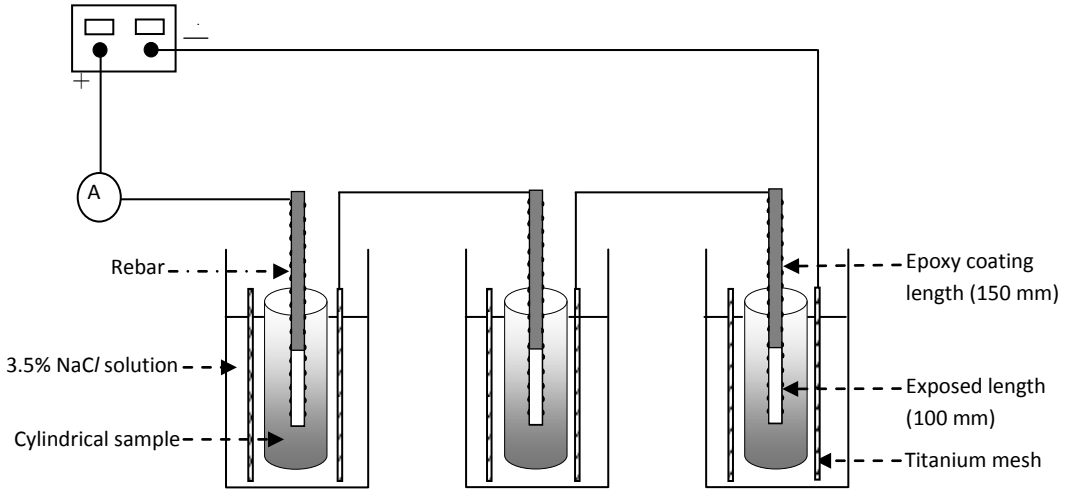

Figure 1. Illustration of accelerated corrosion test

Accelerated Corrosion Test. Fig. 3 illustrates the corrosion rate of the specimens. It indicates that the corrosion rate of specimens made with fibers exhibited a decreasing trend in the corrosion rate proportional to the added polyolefin fibers. Ultrafine slag powders and silica fume made the composites dense enough to prevent the penetration of chlorine ions that would otherwise result in the corrosion of rebar. The addition of both SCMs and polyolefin fibers can arrest the crack propagation and slow the corrosion rate effectively. Inclusion of SCMs in the fiber cement-based composites likely transformed quickly into dense calcium silicate hydrate, filling up the interstitial spaces between the matrix and aggregates and forming a dense, strong, and relatively impermeable composite.

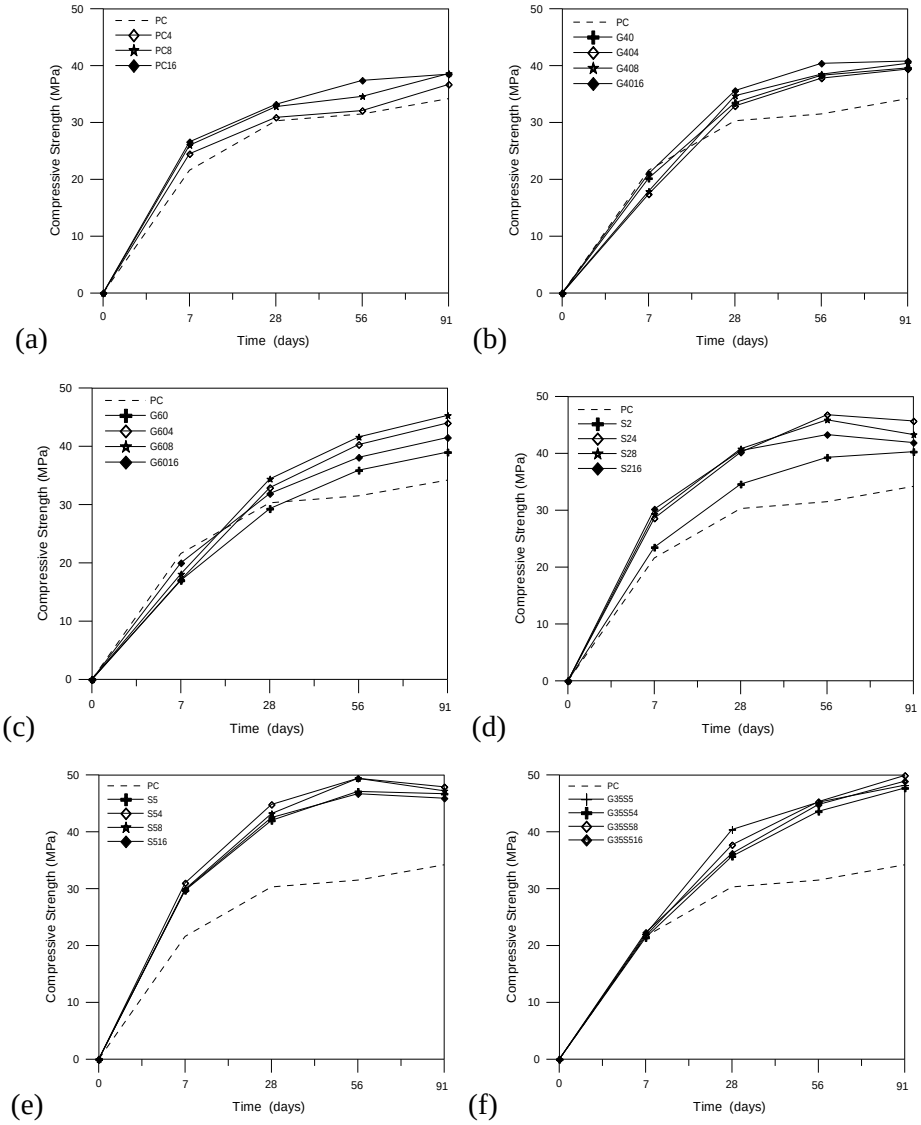

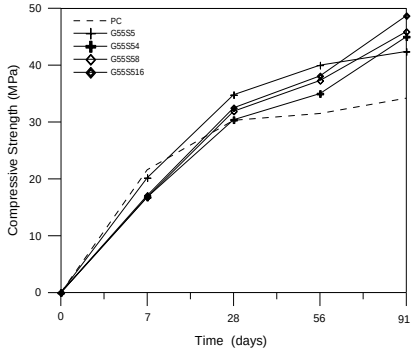

(g)

Figure 2. Compressive strength development curves (a) PC series (b) G40 series (c) G60 series (d) S2 series (e) S5 series (f) G35S5 series (g) G55S5 series

Introducing fibers also attenuated the internal stress in composites resulting from rebar corrosion, which evidently reduced the corrosion rate by inhibiting corrosion product expansion. However, the specimens combining slag and silica fume enhanced better corrosion resistance than other specimens containing individual constituents of slag, silica fume or fibers.

In addition, the specimens combining fibers with slag and silica fume performed worse corrosion resistance than the specimens combining slag and silica fume, but performed better corrosion resistance than the specimens containing individual constituents of slag, silica fume or fibers. It's due to that the distribution of polyolefin fibers cannot be controlled, and there remains the possibility of creating interconnected pore structures, which would accelerate the corrosion of rebar.

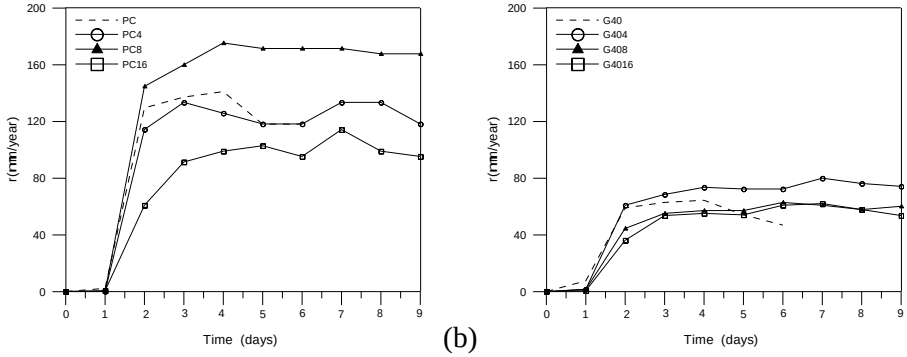

(a)

(b)

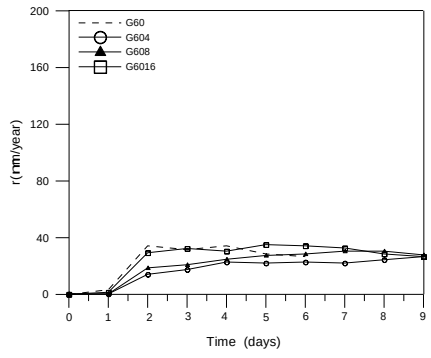

(c)

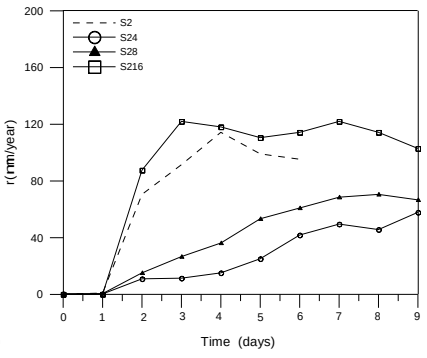

(d)

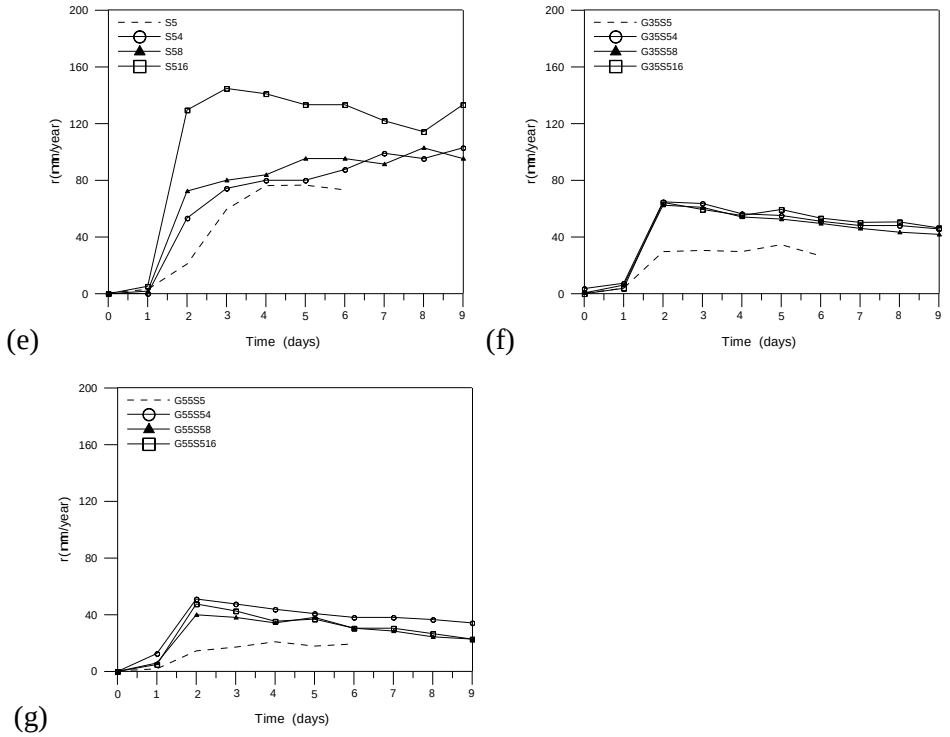

Figure 3. Corrosion rate curves (a) PC series (b) G40 series (c) G60 series (d) S2 series (e) S5 series (f) G35S5 series (g) G55S5 series

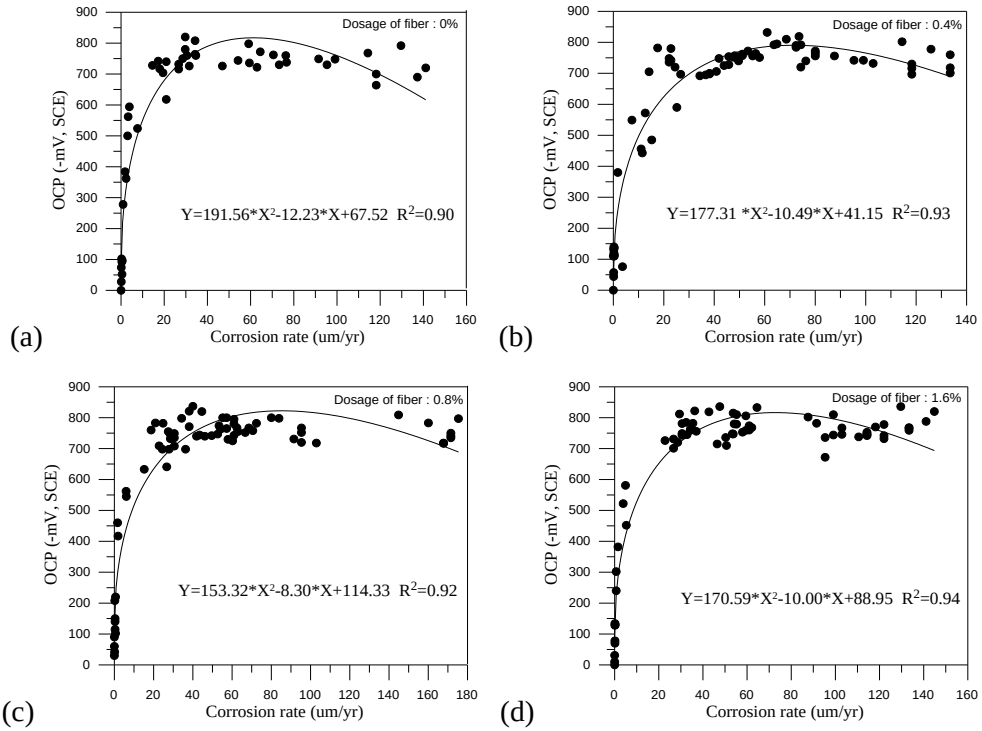

Figure 4. Relationship between OCP and corrosion rate (a) 0 % fiber series (b) 0.4 % fiber series (c) 0.8 % fiber series (d) 1.6 % fiber series

By a linear regression analysis, the good correlations were found between OCP and corrosion rate as presented in Fig. 4. Considering the inclusion of polyolefin fibers, composites with a combined addition of 55 % slag, 5 % silica fume and 0.8 % polyolefin fiber had the lowest corrosion rate.

Table 4. First critical time for the specimens (hr)

Mix no.	PC	PC4	PC8	PC16	G40	G404	G408	G4016
First critical time	2.3	2.5	2.3	1.5	4.8	4.7	5.0	5.0
Mix no.	G60	G604	G608	G6016	S2	S24	S28	S216
First critical time	5.3	1.7	6.0	5.5	2.3	5.3	5.3	2.7
Mix no.	S5	S54	S58	S516	G35S5	G35S54	G35S58	G35S516
First critical time	4.7	4.7	3.7	4.2	5.5	6.5	12.5	13.3
Mix no.	G55S5	G55S54	G55S58	G55S516				
First critical time	4.5	9.5	11.3	1.4				

Impressed Voltage Corrosion Test. The corrosion current curves are presented in Fig. 5. According to the NT BUILD 356-89 code, the definition of the first critical time is the expansive corrosion products leading to strain of mortar, starting from corrosion initiation up to visible creaking (Caré, 2007). Table 4 gives the first critical time in the impressed voltage corrosion test. The first critical time increased significantly with an increase in the SCMs and fiber content, which would decelerate the corrosion of rebar. It is also noticed that the corrosion current decreased and deterioration occurrence times extended with the usage of SCMs and fiber, which validates the results of accelerated corrosion test to compare different mixtures.

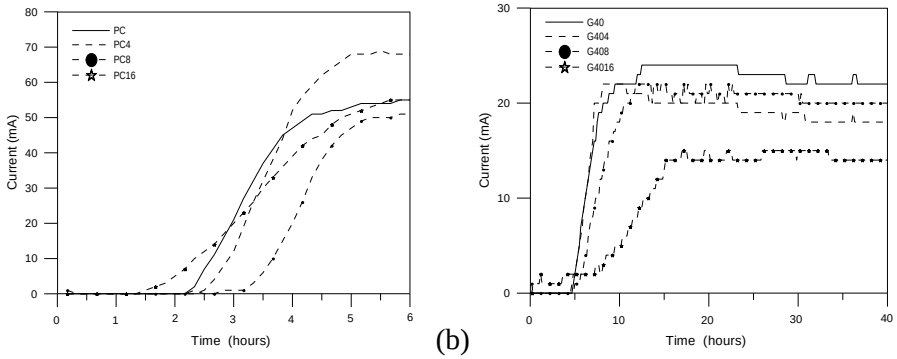

(a) (b)

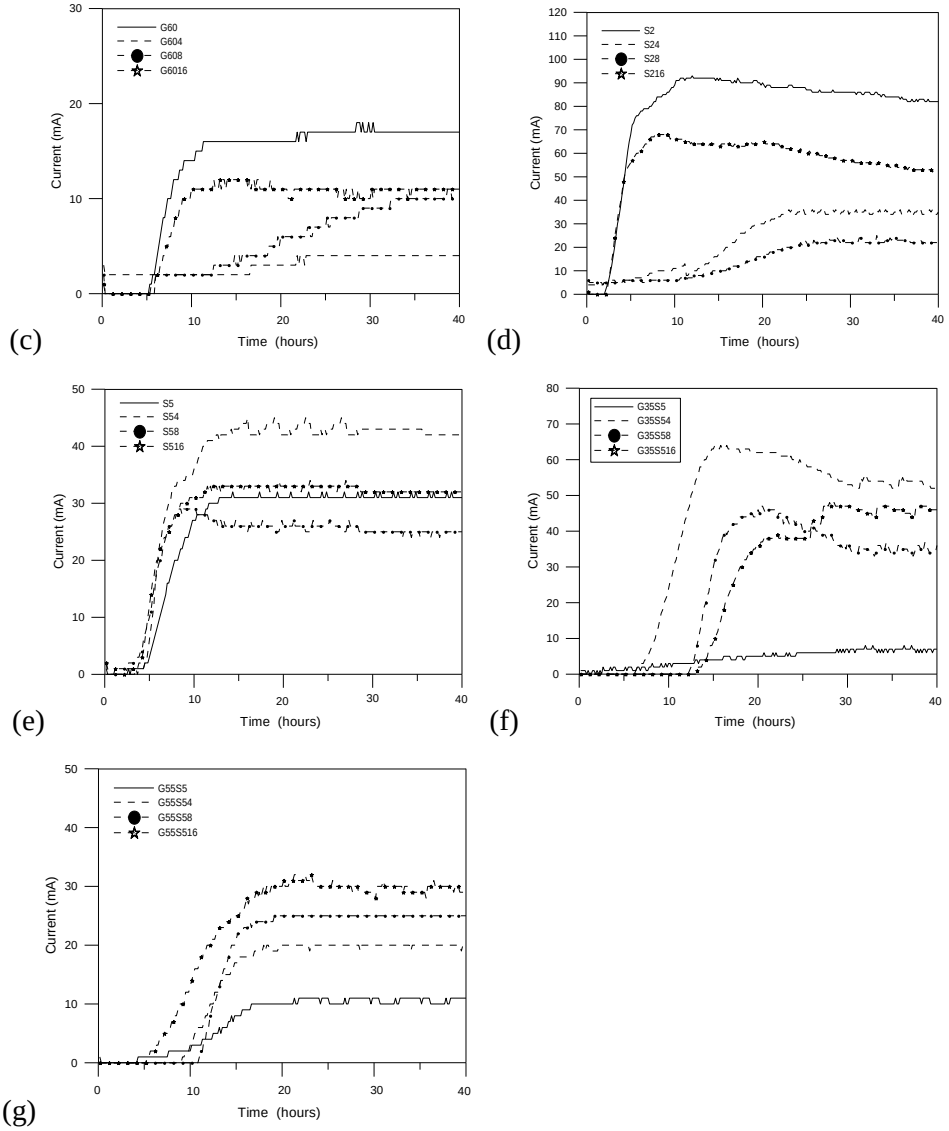

Figure 5. Corrosion current curves (a) PC series (b) G40 series (c) G60 series (d) S2 series (e) S5 series (f) G35S5 series (g) G55S5 series

However, the improvements in the corrosion resistance of cement-based composites obtained by the combination of ultrafine slag, silica fume and polyolefin fiber were attributed to changes in the porosity nature and microstructure of the hardened paste. The superior bonding between fiber and matrix, and dense microstructure of composites can limit the movements of aggressive ions toward the surface of embedded reinforcing steels. Thus, the G55S58 specimens also performed better corrosion resistance in the series.

CONCLUSIONS

The inclusion of polyolefin fiber, ultrafine slag and silica fume effectively improved the compressive strength and corrosion resistance. The combination of slag and silica fume ranked first; the combination of three kinds of additives; fiber with slag and silica fume, ranked second; the combination of fiber and one kind of SCMs ranked third; the individual addition of fiber, slag and silica fume ranked last. The specimens containing fibers with slag

and silica fume performed worse corrosion resistance than the specimens containing slag and silica fume due to the poor distribution of polyolefin fibers in the composites. Considering the advantage of fiber cement-based composites, the combination of 55 % ultrafine slag, 5 % silica fume and 0.8 % polyolefin fibers provided the best corrosion resistance in this study.

REFERENCES

Asokan, P., and Osmani, M. (2010). "Improvement of the mechanical properties of glass fibre reinforced plastic waste powder filled concrete." *Const build mat*, 24(4): 448-460.

Caré, S., and , Raharinaivo A. (2007). "Influence of impressed current on the initiation of damage in reinforced mortar due to corrosion of embedded steel." *Cem Concr Res*, 37(12): 1598-1612.

Chalioris, C. E., and Karayannis, C. G. (2009). "Effectiveness of the use of steel fibres on the torsional behaviour of flanged concrete beams." *Cem Concr Compos*, 31(1): 331-341.

Han, H. Y., Lin, W. T., Cheng, A., Huang, R., and Huang, C. C. (2012). "Influence of Polyolefin Fibers on the Engineering Properties of Cement-based Composites Containing Silica Fume." *Mater Des*, 37: 569-576.

Kang, S. T., Lee, B. Y., Kim, J. K., and Kim, Y. Y. (2011). "The effect of fibre distribution characteristics on the flexural strength of steel fibre-reinforced ultra high strength concrete." *Const build mat*, 25(5): 2450-2457.

Lee, C. L., Huang, R., Lin, W. T., and Weng, T. L. (2012). "Establishment of the Durability Indices for Cement-based Composite Containing Supplementary Cementitious Materials." *Mater Des*, 37: 28-39.

Lin, W. T., Huang, R., Lee, C. L., Hsu, H. M. (2008). "Effect of Steel Fiber on the Mechanical Properties of Cement-based Composites containing Silica Fume." *J Mar Sci Tech*, 16(3): 214-221.

Passuello, P., Moriconi, G., and Shah, S. P. (2009). "Cracking behavior of concrete with shrinkage reducing admixtures and PVA fibers." *Cem Concr Compos*, 31(10): 699-704.

Şahin, Y., and Köksal, F. (2011). "The influences of matrix and steel fibre tensile strengths on the fracture energy of high-strength concrete." *Const build mat*, 25(4): 1801-1806.

Sahmaran, M., and Li, V.C. (2009). "Influence of Microcracking on Water Absorption and Sorptivity of ECC." *Mater Struct*, 42(5): 593-603.

ASTM G59 (2003). "Standard test method for conducting potentiodynamic polarization resistance measurements." American Society for Testing and Materials, ASTM specification, Philadelphia.

Stern, M., and Geary, A.L. (1957). "Electrochemical polarization." *J Electrochem Soc*, 104(1): 56-63.